The distribution of Silicon in soil is influenced by termite bioturbation in South Indian forest soils

Pascal Jouquet, Floriane Jamoteau, Sabyasachi Majumdar, Pascal Podwojewski, Prakash Nagabovanalli, Laurent Caner, Doris Barboni, Jean-Dominique Meunier

The distribution of Silicon in soil is influenced by termite bioturbation in South Indian forest soils

Pascal Jouquet[a,b,*], Floriane Jamoteau[a,b,c], Sabyasachi Majumdar[d], Pascal Podwojewski[a], Prakash Nagabovanalli[d], Laurent Caner[e], Doris Barboni[c], Jean-Dominique Meunier[c]

Adresses

[a] *Sorbonne Université, UPEC, CNRS, IRD, INRA, Institut d'écologie et des sciences de l'environnement, IESS-Paris, F-93143 Bondy, France*

[b] *Indo-French Cell for Water Science (IFCWS), Indian Institute of Science, Bangalore, Karnataka, India*

[c] *CEREGE, CNRS, Aix-Marseille University, IRD, INRA, 13545 Aix-en-Provence, France*

[d] *Department of Soil Science & Agril. Chemistry. University of Agricultural Sciences. GKVK, Bangalore 560 065 Karnataka, India*

[e] *Université de Poitiers, Institut de Chimie des Milieux et Matériaux de Poitiers, IC2MP UMR 7285 CNRS, 5 rue Albert Turpain, TSA51106, 86073 Poitiers cedex 9, France*

* Corresponding author: pascal.jouquet@ird.fr

ABSTRACT

Si is one of the most abundant element on earth and an abundant literature shows its beneficial effects on plant growth and resistance. We here question the influence of termites, as key soil bioturbators, on the distribution of Si in a tropical soil. The abundance and forms of Si in termite mounds build by *Odontotermes obesus* (TM) or in the soil eroded from TM but redistributed on the ground surface (EROD) were compared to those measured in the 0-5 ($Ctrl_{0-5}$) and 70-120 cm soil layers ($Ctrl_{70-120}$). Although termites use the soil from $Ctrl_{70-120}$ for building their mounds, we found that TM and EROD had intermediate soil physical, chemical and mineralogical properties between $Ctrl_{0-5}$ and $Ctrl_{70-120}$. Clay content was not significantly different between soil materials. However, the lower variability measured in TM than in the soil suggested that termites used soil layers with higher amounts of clay fraction and with a preference especially for layers enriched in 2:1 clay minerals (smectite) most likely because they provide better physical properties in terms of plasticity and water retention than kaolinite. Finally, phytoliths and bioavailable Si (Si_{CC}) contents were increased in TM in comparison with $Ctrl_{70-120}$, suggesting an incorporation of phytoliths in termite construction through their saliva and/or an increasing availability of Si_{CC} from the minerals. In conclusion, this study highlights how termites, through their feeding and building activities, impact Si distribution in tropical soils.

Keywords: Si, clay, mineralogy, phytoliths, bioturbation, soil profile

1. Introduction

Silicon (Si) is the second most abundant element in the earth's crust after oxygen, with approximately 28 and 47% of its mass, respectively (Singer and Munns, 1999). It is not included in the list of elements essential for plants but there is an abundant literature showing its beneficial effects on the resistance of plants to parasites and drought (Liang et al., 2015; Datnoff et al., 2001).

In soil Si is a major constituent of parent rock minerals (such as quartz, feldspars) and of secondary minerals originated from pedogenesis, such as clay minerals and amorphous silica. Biogenic amorphous silica particles can also be found in soil as plant and microorganism remains, i.e., phytoliths (Cornelis and Delvaux, 2016) and diatom frustules or thecamoebian tests (Sommer et al., 2006). These amorphous silica particles can play an important role in the cycling of Si because they constitute a pool of highly reactive silica (Fraysse et al., 2009). Large fauna like grazers can also affect the cycling of Si through the accelerating transfer of plant Si to aquatic environments (Schoelynck et al., 2019) or through the increase production of biogenic silica (Melzer et al., 2010). The amount and quality of the different Si pools vary also with soil depth. Soil horizons are usually identified by different clay contents and minerals while phytoliths are usually concentrated in the topsoil and their content rapidly decreases with depth (Alexandre et al., 1997). The pool of Si extracted by 0.01 M $CaCl_2$ (Si_{CC}) is used to estimate the Si immediately available for plants (Haysom and Chapman, 1975). The distribution of Si_{CC} along soil profile may increase with depth and be associated with the clay fraction (Vandevenne et al., 2015). Another pool considered bioavailable for plant is the pool of Si adsorbed on the surface of minerals estimated by 0.05 M acetic acid extraction (Si_{AA}) (Sauer et al., 2006). Si_{AA} seems to be controlled by oxides and clay minerals and may also increase with depth (Cornelis et al., 2011 PLSO; Vandevenne et al., 2015). Surprisingly and despite their importance in the cycling of nutrients, the impact of soil macrofauna on Si dynamic has been poorly documented, with the exception of a recent article focusing on earthworms (Georgiadis

et al., 2019), and there is a dearth of information on how soil macrofauna impacts clay mineralogy and the availability of Si for plants.

Amongst the soil macrofauna, organisms from the soil engineering group (*sensu* Lavelle et al., 1997) impact soil functioning at different spatial and temporal scales (Bottinelli et al., 2015). This role is played by termites in tropical dryland ecosystems, and especially by termites from the fungus-growing functional group (Macrotermitinae subfamily) in Africa and Asia (Jouquet et al., 2016). Termites are key decomposers of the litter in tropical environments (Amadou Issoufou et al., 2019) and their building activity is associated to the redistribution of soil organic matter and elements in their biomass and organo-mineral constructions. Studies carried out in Africa and Asia showed that fungus-growing termites impact the distribution, the type of clay minerals (kaolinite vs. smectite) and the mineralogical properties of phyllosilicates (Jouquet et al., 2002, 2007). Termites are also known to impact the dynamic of Si at the profile scale through the selective use of material coming from the deep soil layers within their nests, then resulting in the redistribution of clay minerals and elements (Holt and Lepage, 2000; Abe et al., 2012; Mujinya et al., 2010, 2011, 2013; Erens et al., 2015). However, the depth at which termites fetch the clay particles remains mostly unknown and termite bioturbation and the upward translocation of soil from the deeper layers to the surface are likely to be associated with a redistribution of Si_{CC} and Si_{AA} pools in termite mounds and thereafter in the surrounding soil environment with the erosion of termite mounds.

In Southern India, the termite species *Odontotermes obesus* is known to play an important role in the decomposition of litter (Shanbhag and Sundararaj, 2013) and its mounds are conspicuous features of the landscapes (Shanbhag et al., 2017). These mounds are especially abundant in protected areas such as in the deciduous forests of the Bandipur Tiger Reserve. In this environment termite mounds have specific soil physical and chemical properties (Jouquet et al., 2017a) and a recent study showed that they are mainly made of soil collected between 70

to 120 cm depth (Jouquet et al., 2017b). The aim of this study was therefore to determine the impact of *O. obesus* bioturbation on the distribution of Si in soil. Our hypothesis was that termite feeding and building activities (i.e., the construction of mounds from material selected in the deep soil layers) participate in a selective redistribution of clay minerals, phytoliths and available Si (Si_{CC}), which are thereafter redistributed to the soil surface.

Material and Methods

Study site

Soils were sampled in the Mule Hole experimental watershed (4.1 km^2). This dry deciduous forest is located in the Bandipur Tiger reserve in Southern India at 11°44′N and 76°26′E (Chamarajanagar district, Karnataka state). The Mule Hole watershed is located in the sub-humid zone of the sharp climatic gradient induced by the Western Ghats. As a result of the short-term variability of the South-West Monsoon, the experimental watershed is characterized by rainfall ranging from 1000 to 1500 mm yr^{-1}, usually concentrated during the monsoon from June to August and from October to November. The mean annual temperature is 27°C (Braun et al., 2009). The elevation of the watershed ranges from 820 to 910 m a.s.l. The relief is mostly undulating with gentle slopes. The soil cover of the watershed has been mapped by Barbiero et al. (2007) based on the FAO terminology (IUSS-Working-Group-WRB, 2015). Parent rocks consist of peninsular gneiss intermingled with much less abundant mafic to ultramafic rocks, mostly amphibolite. Soil depth is variable but ranging from 1 to 3 m in average (Barbiero et al., 2007; Braun et al., 2009). The main soil types are Ferralsols and Chromic Luvisols, with clay mineralogy dominated by kaolinite (1:1 clay) and characterized by an accumulation of iron and aluminum oxides. The soils have less than 20 g kg^{-1} of C in the first soil layer and < 10 g kg^{-1} below 20 cm depth. The clay content ranges from 30 to 40% and clays minerals are also dominated by 1:1 clays (kaolinite) (Jouquet et al., 2016b). The vegetation is a dry deciduous forest. In this environment, cathedral-shaped termite mounds are built by *O. obesus* (Chhotani

and Bose, 1979; Jouquet et al., 2016a,b, 2017a) (Figure 1). The soil of termite mounds has similar clay contents but it is impoverished in C (0.54-fold) in comparison with the surrounding topsoil (Jouquet et al., 2016, 2017a,b).

Soil sampling

Termite mounds built by *O. obesus* vary considerably in size (Shanbhag et al., 2017) and only large mounds from 1.5 to 1.8 m high and > 0.5 m^3 were considered in this study. Samples were collected from the outer-wall of three termite mounds (TM) and from their periphery in a distance of about 15 cm (impacted by mound erosion, EROD). Soils were also sampled in the surrounding soil environment (control) in a distance > 5–10 m ahead of the mounds in taking into account the gentle slope of the watershed (not impacted by mound erosion) at several soil depths down to 4.0 m in three different locations (n = 39). Data were grouped according to their depths ($Ctrl_{0\text{-}5}$: 0–5 cm, $Ctrl_{70\text{-}120}$: 70-120 cm) with the assumption that termites collect the soil mainly from the 70-120 cm soil layer for building their mounds (Jouquet et al., 2017b).

Analysis of soil properties

The soil physical properties measured included the particle-size distribution, after destruction of organic matter and dispersion with sodium hexametaphosphate (AFNOR, NFX 31 107): clay (< 2 µm) and silt (2–50 µm) were obtained by pipette method and sand (50–2000 µm) by sieving. To assess Soil Organic Matter (SOM) content, the C and N concentrations were measured using an elemental analyzer Flash 2000 HT. The cationic exchange capacity and the content of exchangeable cations (Ca, Mg, Na, K, Fe, Mn and Al) were determined at soil pH by exchange with cobaltihexamine (AFNOR, NF ISO 23470). The amount of SiO_2, Fe_2O_3 and Al_2O_3 were measured by ICP-OES after fusion with lithium metaborate $LiBO_2$ and subsequent dissolution in a mixture of HNO_3 (1 mol L-1), H_2O_2 (0.5 % v/v) and glycerol (10 % v / v) at the

144 CNRS Service d'Analyse des Roches et des Minéraux (SARM) (Carignan et al., 2001). All
145 these analyses were carried out on soil aggregates >2 mm that were ground before analyses to
146 homogenize the material.
147
148 *Si pools and phytoliths*
149 Plant available Si was measured in comparing the pools of readily soluble Si extracted by 0.01
150 M $CaCl_2$ (Si_{CC}, Haysom and Chapman, 1975) and the pool of adsorbed Si extracted by 0.5 M
151 acetate-acetic acid (Si_{AA}, Korndörfer and Lepsch, 2001; Narayanaswamy and Prakash, 2009,
152 2010). Phytoliths were extracted using HCl (33%) to remove carbonates, 2/3 nitric plus 1/3
153 perchloric acid to remove organic matter. Soil clays were removed by repeated decantations,
154 and separation of biogenic silica particles from heavy minerals was achieved by densimetric
155 separation using $ZnBr_2$ set at d = 2.3 g cm^{-3}. The extracts were weighted and phytoliths were
156 mounted on slides for observation under optical microscope. More than 250 phytoliths were
157 counted per sample. Morphotypes with clear taxonomical identification were silica short cell
158 phytoliths (rondel, bilobate, polylobate and cross) from Poaceae (grasses), spheroid psilate and
159 decorated from woody dicotyledons (considered forest indicator phytoliths), and spheroid
160 echinate from Arecaceae (palms). Other phytoliths included bulliform flabellate, acute bulbosus
161 (silicified hair cells), and various elongate and blocky morphotypes which were mostly non-
162 diagnostic (International Code for Phytolith Nomenclature, 2019). The ratio of spheroid
163 decorated versus the sum of grass silica short cells (or D/P° index) increases with the increasing
164 abundance of trees and shrubs versus grasses and is commonly used to trace the tropical
165 forest/savanna boundary (Bremond et al. 2008). On the same slides, but in a separate counting
166 session we measured the proportion of corroded vs. plain phytoliths to identify the origin of
167 phytoliths with the assumption that phytoliths at depth likely underwent prolonged dissolution

than the more recent phytoliths located at the soil surface following Sommer et al. (2006). Phytoliths relative abundance were calculated based on the total phytolith sums.

Clay mineralogy

Clay mineralogy from termite mound soil samples (TM and EROD) was compared to the mineralogy of the soil at 0-5 and 70-120 cm depths ($Ctrl_{0-5}$ and $Ctrl_{70-120}$) (n = 3 per treatments). Clay mineralogy was determined after extraction of the clay size fraction (particles < 2 µm) from the bulk soil samples. The fractions < 50 µm were obtained by wet sieving and then dispersed into 1 mol L^{-1} NaCl (five saturations) and ultrasonication. The < 2 µm fractions were obtained by sedimentation and were subsequently flocculated and saturated with 0.5 mol L^{-1} $CaCl_2$ (Caner et al., 2014). XRD patterns of oriented preparations were recorded in the air-dried state (Ca-AD) and after saturation with ethylene glycol (Ca-EG) to identify the clay minerals (Caner et al., 2014). Since no additional information was obtained from the saturation with ethylene-glycol, only results from the Ca-AD preparation was shown. The X-Ray diffraction patterns were decomposed into elementary peaks (Lanson, 1997) using Fityk software over the 3-14°2θ range. The procedure included removal of baseline and decomposition of the signal into Gaussian elementary curves. The diffractograms were fitted with the minimum curves to obtain a reliable fit of the experimental pattern. The parameters of the elementary curves (position, full-width at half maximum – FWHM and maximum intensity, surface area) were used to identify the soil clay mineral (kaolinite, illite, smectite, mixed layers illite/smectite) species according to Righi et al. (1995) and Velde (2001). A semi-quantitative phase analysis was performed using the relative surface peak area of each peak of clay minerals over the sum of the peak surface areas. The relative surface peak area of each peak does not correspond to the proportion of the respective mineral, however, the variations of relative surface areas correspond to variations in mineral quantities if the samples comes from the same sequence

193 (Lanson 1997). Peaks at ~7.20 and 7.30-7.40 Å were attributed to kaolinite (K). The peak of
194 illite at ~10 Å was decomposed into well crystallized illite (WCI) at 10.0 Å and poorly
195 crystallized illite (PCI) at 10.2-10.4 Å. The peaks at ~15 Å in AD state that displace to ~17 Å
196 were attributed to smectite (S) and the peaks between 10 and 15 Å in AD state that displaced
197 between 10 and 17 Å in EG were attributed to mixed layers illite/smectite with variable
198 proportion of the two components.
199
200 *Statistical analyses*
201 Residues were tested for normality of variance using the Shapiro–Wilk test and log10-
202 transformed if required. Soil chemical and physical properties were analyzed by analysis of
203 variance (ANOVA) with treatments as independent variables. LSD tests were then performed
204 to assess differences between means. Post-hoc planned pairwise comparisons were performed
205 by Wilcoxon–Mann–Whitney U tests when parametric ANOVA were impossible to use, even
206 after data transformation. Impact of the treatments on soil variables and soil mineralogy were
207 analyzed using a principal component analysis (PCA). Correlations between variables and the
208 amount in Si_{CC}, Si_{AA} and phytoliths were carried out using the spearman test. 95% confidence
209 intervals associated to the percentages in phytoliths and 99% confidence intervals associated
210 with the D/P° ratios were calculated following Suchéras-Marx et al. (2019). All statistical
211 parameters were calculated using R studio and R version 3.2.1 with ade4, factoextra,
212 factoMineR and corrplot packages. Differences among treatments were declared significant at
213 the 0.05 probability level.
214
215 **Results**
216 *Difference in soil chemical and physical properties*
217 The chemical properties of the 4 soil materials are shown in Table 1 and a PCA-projection of
218 the samples from significant variables is shown in Figure 1. Soil materials were mainly

219 differentiated along the first axis while the variability within the samples was evidenced on the
220 second axis, which explained 63.0 and 18.5% of the total variability, respectively. Samples
221 varied from the soil surface ($Ctrl_{0-5}$) to TM, EROD and finally $Ctrl_{70-120}$. No significant
222 difference in soil particle size fractions, in pH and in exchangeable Mg^{2+} and K^{+} contents could
223 be measured between the four soil materials ($P > 0.05$ in all cases) (Table 1). $Ctrl_{0-5}$ was
224 enriched in C and N and characterized by a greater CEC and exchangeable Ca^{2+} content but
225 lower exchangeable Al^{3+} content in comparison with the other treatments. Conversely, $Ctrl_{70-120}$
226 were impoverished in C and N but enriched in exchangeable Na^{+}, Al_2O_3 and Fe_2O_3 in
227 comparison with the other soil materials. In general, TM and EROD had intermediate properties
228 in comparison with the $Ctrl_{0-5}$ and $Ctrl_{70-120}$ (Figure 1) and no significant difference occurred
229 between them, with the exception of the concentration in exchangeable Mn^{2+} that was similar
230 in TM and $Ctrl_{70-120}$ but higher than in EROD and $Ctrl_{0-5}$ ($P > 0.05$ between them, Table 1).
231 Figure 2 shows the evolution of clay content in TM and EROD and at different soil depths. The
232 amount of clay was highly variable (e.g. from < 10 to > 50% at 150 cm depth), especially in
233 comparison with the clay content in TM and EROD. Despite this high variability, an increase
234 in clay content was measured at about 50-150 cm depth.
235
236 *Si pools and phytoliths*
237 Figure 3 shows that the proportion of SiO_2 and the amount of Si_{CC} were the lowest in $Ctrl_{70-120}$,
238 without any significant difference between the other treatments ($P > 0.05$). Conversely Si_{AA}
239 content was the highest in $Ctrl_{70-120}$ and the lowest in $Ctrl_{0-5}$ while TM and EROD had
240 intermediate positions. The proportion of phytoliths was low with percentages < 1%. The
241 highest value was measured in $Ctrl_{0-5}$ in comparison with $Ctrl_{70-120}$ and TM ($P < 0.05$ in both
242 cases). Conversely, the lowest value was measured in $Ctrl_{70-120}$ in comparison with $Ctrl_{0-5}$ and
243 EROD ($P < 0.05$ in both cases). TM and EROD had a similar percentage of phytoliths with

intermediate values in comparison with the two control soils. Si_{CC} was not correlated with the soil physical and chemical properties, with the exception of a positive correlation with phytoliths ($P = 0.028$) and Mg^{2+} ($P = 0.017$). Conversely, Si_{AA} was negatively correlated with the amounts in C, N, the CEC and Si:Al ratio ($P = 0.048$, 0.048, 0.049 and 0.013, respectively) but positively correlated with the total amount in Al_2O_3 ($P = 0.013$). Moreover, the amount in phytoliths was positively correlated with the CEC and the amounts in C, N, Ca^{2+}, Mg^{2+} and Si_{CC} ($P = 0.001$, 0.008, 0.008, 0.001, 0.001 and 0.028, respectively) but negatively correlated to the amount in Fe^{3+} and Al^{3+} ($P = 0.018$ and 0.011, respectively).

Identification of the phytoliths shows that most of them came from grasses and woody dicotyledons (trees and shrubs), with little differences in the phytolith-inferred vegetation signal between $Ctrl_{0\text{-}5}$ and $Crtl_{70\text{-}120}$, but strong difference with TM. In TM, phytolith pool was essentially coming from grasses (phytolith ratio Dicotyledons:Poaceae, D:P° < 0.7), while it was coming from woody plants in the Crtl samples (D:P° > 2) (Figure 4 and see appendix A for the detailed phytolith counts). A gradient of corrosion was observed from the top-soil to the deeper soil layers with a dominance of non-corroded phytoliths in $Ctrl_{0\text{-}5}$, a dominance of corroded phytoliths in the 90-100 cm soil layer and intermediate values in the 20-40 cm soil layer (Figure 5). In TM, phytoliths had intermediate proportion of corroded phytoliths than between the 0-5 and 20-40 cm soil layers (Figures 5 and 6).

Variation in clay abundance and mineralogy with soil depth

Differences in clay mineralogy between soil samples are shown in Figure 7. Soil materials were mainly differentiated by the second axis, which explained 30% of the total variability. Samples from the topsoil were enriched in smectite (S) and poorly crystallized illite (PCI) in comparison with soil sampled below 70 cm depth that were rich in kaolinite (K). TM and EROD had the

same signatures and intermediate properties between those of the soils sampled in $Ctrl_{0-5}$ and $Ctrl_{70-120}$.

Discussion

Bioturbation and translocation of clay

Bioturbation and the edification of termite mounds by fungus-growing termites is associated with a translocation of soil material from the deeper soil layers to the surface. Usually evidenced by an enrichment in clay particles or the presence of minerals that are less abundant than in the topsoil, this process of translocation as well as the depth at which termites collect the soil remain poorly quantified. In a recent study, we showed that the soil from the outer-wall of *O. obesus* mounds mainly comes from the ~ 70 to 120 cm soil layer (Jouquet et al., 2017b). Here, measure of the percentage of clay fraction in soil did not evidence a significant difference between soil materials, mainly because of the high variability in clay content along the soil profile. This variability in clay content was reduced in termite mound soils, showing a possible regulation of the amount of clay fraction in soil by termites for strengthening cohesion between aggregate and ensuring the resistance of TM, as evidenced in laboratory conditions (Jouquet et al., 2002, Oberst et al., 2016) and for a better control of their habitat and resistance to predators (Jouquet et al., 2006).

Si available pools

The 0-5 cm soil layer was enriched in SiO_2 in comparison with the 70-120 cm soil layer, which was enriched in Al_2O_3 content (see the supplementary file 1 showing the higher concentration in Al_2O_3 at this soil depth). Phytoliths in the 70-120 cm soil layer were also less abundant and more corroded than in the topsoil in a good agreement with previous observations (Alexandre et al., 1997; Sommer et al., 2006). Indeed, the dynamic of phytoliths in soil results from burial, illuviation and bioturbation processes and phytoliths from deeper horizons are usually less

294 abundant, older and more corroded than in the surface (Sommer et al. 2006; White et al., 2012).
295 A similar amount of phytoliths was measured in TM and in the topsoil while EROD had
296 intermediate phytolith contents between TM and $Ctrl_{70\text{-}120}$. Difference in D:P° ratio between
297 TM and Ctrl soils also shows that TM contained more phytoliths from grasses than control soil
298 samples. Although this study does not allow to reject the assumption that phytoliths from deeper
299 soil layers were selectively incorporated into TM, we consider this hypothesis unlikely since
300 this would have resulted in higher representation of forest indicator phytoliths, as forest is the
301 dominant vegetation at Mule Hole (Riotte et al., 2018). Moreover, phytolith morphotypes vary
302 in size but grass silica short cell phytoliths and the forest indicator spheroids are in the same
303 size range (8-30 microns). It is therefore unlikely that grass phytoliths were incorporated in TM
304 because they were smaller and because they were differently associated to clay particles.
305 Despite the fact that *O. obesus* can feed on a variety of litter components (e.g. elephant dung,
306 wood and leaves) (Cheik et al., 2018, 2019; Shanbhag et al., 2019), grasses are mostly
307 consumed by herbivores in Mule Hole catchment. The presence of grass phytoliths in TM
308 therefore suggests that termites act as primary decomposers of herbivore dungs in the studied
309 area. This hypothesis is in line with recent studies carried out in southern India which showed
310 that elephant dung material is very attractive to termites which prefer this material over carton,
311 wood or leaves (Cheik et al., 2018, 2019; Shanbhag et al., 2019). Indeed, despite inhabiting
312 forested environments in Karnataka and the Nilgiri Region, elephants preferentially feed on
313 Panicoideae grasses which constitute more than 84% of their annual bulk diet (Baskaran et al.
314 2010). A large amount of these grasses is only partially decomposed, making this material very
315 attractive to termites. Therefore, if the consumption of grasses is associated with a partial
316 digestion of organic matter by termites for building their biomass and ensuring their activity,
317 the Si contained in the phytoliths is not used by termites. From these findings we suggest that
318 termites incorporate phytoliths in their constructions most likely when they moisten the soil

aggregate pellets with saliva and potentially faeces. This hypothesis is consistent with the presence of monosaccharides from plant origin in the epigeous nest of fungus-growing termites (Sall et al., 2002) and the higher C content measured in TM in comparison with $Ctrl_{70\text{-}120}$ and the positive correlation between phytoliths and the C content. Moreover, since phytoliths were mainly non-corroded phytoliths in TM, we even suggest that phytoliths resist to termite and microbial (including *Termitomyces* sp.) metabolisms.

Si_{CC} and Si_{AA} were respectively higher and lower in the topsoil layer in comparison with $Ctrl_{70\text{-}120}$. Interestingly, despite the fact that TM was mainly built from the soil at 70-120 cm depth, TM had a closer signature with the topsoil than with the deeper soil with similar amounts of SiO_2, Si_{CC} and Si_{AA}. Although this study does not allow to disentangle the mechanisms associated to this change in Si pools, the positive correlation between Si_{AA} and the amount of Al_2O_3, but not the amount in clay, and the positive correlation between Si_{CC} and phytoliths suggest either (i) a total reorganization of the structure of soil pellets and a decrease in the interactions between Si and oxides and a shift from Si_{AA} to Si_{CC}, (ii) a production of Si_{CC} from phytolith dissolution, and/or (iii) a selection of particles from $Ctrl_{70\text{-}120}$ that were impoverished in oxides (see supplementary file 2) but enriched in clay and Si_{CC}. Another explanation could be that the dissolution of 2:1 clay minerals, mainly found on the topsoil and TM, increases the Si_{CC} pool, even if this process is likely to be limited with a soil pH > 6. This explanation is in line with Violette et al. (2010) who found that the dissolution of smectite provides large amount of dissolved silica (i.e., 75% of the export of dissolved silica) in the study watershed.

Modification in clay mineralogy

The 70-120 cm soil layer was characterized by a higher percentage of clay fraction and higher contents in kaolinite and Al_2O_3 that are characteristics of kandic horizons (Brady and Weil, 1999; Soil Survey Staff, 2014). The presence of the kandic horizon was confirmed with the X-

344 ray diffraction data that revealed the presence of smectites and poorly crystallized illite (i.e. 2:1
345 phyllosilicates) in the topsoil and on the contrary a mineralogy dominated kaolinite (1:1
346 phyllosilicate) in the kandic horizon. The presence of smectite on the topsoil was unexpected
347 and suggests a high level bioturbation activity with the upward movement of soil and
348 neoformation processes. The concentration of Mn^{2+} in soil solutions is largely controlled by
349 oxidation and reduction reactions and the higher concentration of this cation in the kandic
350 horizon also confirms a process of accumulation at this soil depth. Therefore, similar
351 concentration in Mn^{2+} between the 70-120 cm soil layer and TM confirms the utilization of soil
352 from the kandic horizon for building termite mounds. However, the lower concentration in
353 Mn^{2+} in EROD is likely to be explained by the high solubility of this cation in solution (Gilkes
354 and McKenzie, 1988) and its rapid leaching from the soil eroded from the mound, despite the
355 fact that this soil is poorly permeable in comparison with the surrounding topsoil (Traoré et al.,
356 2019). Although TM were mainly made of soil coming from the kandic horizon, clay minerals
357 in termite mounds had intermediate properties between those observed in the topsoil and those
358 sampled in the deeper soil layers. Differences in clay minerals or in Si:Al ratio between TM
359 and the surrounding topsoil have been evidenced in different environment (e.g., Wielemaker,
360 1984; Abe et al., 2012). They are usually explained by the use of specific clay minerals and/or
361 the ability of termites to modify the properties of clay minerals (Schaefer, 2001; Jouquet et al.,
362 2011). Since the modification of clay minerals by termites is limited to the swelling ability of
363 2:1 clay minerals (Jouquet et al., 2002; 2007), our results suggest that 2:1 clay minerals may be
364 selected by *O. obesus* for building their nests than kaolinite, most likely because of their better
365 physical properties in terms of plasticity and water retention (Andrade et al., 2011; Spagnoli et
366 al., 2018). Another explanation could be 2:1 clay minerals found in TM could be produced from
367 the dissolution of phytoliths and the interaction between Si_{CC} and kaolinite (Sommer et al.,
368 2006). In a highly weathered Oxisols in the Amazon forest, Lucas et al. (1993) showed that the

369 occurrence of kaolinite, instead of gibbsite, in the topsoil (or surface horizon) was attributed to
370 the resilication of gibbsite by the soluble silica provided by phytolith dissolution. A similar
371 process of resilication of kaolinite could be suggested for the formation of smectite in TM by
372 the biological uplift of cations and highly reactive silica from the dissolution of phytoliths. Over
373 longer period of time, the accumulation of 2:1 clay minerals in TM is likely to be important at
374 the ecosystem scale. Indeed, *O. obesus* mound turnover rate has been estimated to reach a soil
375 turnover of 3.1-31 mm ky^{-1} in the same study site (Jouquet et al., 2017). Since clay minerals
376 accumulated in termite mounds return to the surrounding soil environment after termite mound
377 degradation, further research is needed to determine if the accumulation of this material
378 contributes and/or explains the presence of 2:1 clay minerals in the topsoil.
379
380 *Conclusion*
381 Findings from this study show that *O. obesus* has a significant impact on the distribution of Si
382 in soil. First, we explained the lower variability in clay content in comparison with the high
383 variability measured along the soil profile by the need of termites to control the properties of
384 their nests, i.e., the amount of clay fraction in TM, then highlighting the importance of this
385 material for termites. The higher phytolith content in TM was unexpected but could be
386 explained by termite foraging activity (i.e., the consumption of grasses) and the excretion of
387 phytolith in termite saliva. Higher amount in Si_{CC} was also surprising and raised the question
388 of a possible impact of termites on the interaction between Si and minerals in soil. In
389 perspective, we consider that more research is now needed to better understand the fate of the
390 phytoliths in TM. Further studies are also needed to determine if the increase in Si_{CC} content in
391 TM contribute to explain the presence of 2:1 minerals in termite constructions (Jouquet et al.,
392 2002) and the specific vegetation growing in the vicinity or on termite mounds in Africa (e.g.,

393 Traoré et al., 2015), as well as the utilization of TM soil as amendment for increasing soil
394 fertility (Loko et al., 2017).
395
396 **Acknowledgements**
397 This project was supported by the French Institute for research for development (IRD) through
398 "Allocations de recherche pour une thèse au Sud" (ARTS) grant and data from this study were
399 partially obtained from the ALYSES facility (IRD-UPMC) which was supported by grants from
400 Région Ile de France. The Mule Hole basin is part of the ORE-BVET project (Observatoire de
401 Recherche en Environnement - Bassin Versant Expérimentaux Tropicaux, http://bvet.omp.obs-
402 mip.fr/) supported by the French Institute of Research for Development (IRD), CNRS and
403 Toulouse University. The project also benefited from funding from the Indo-French Cell for
404 Water Science (LMI CEFIRSE, http://www.cefirse.ird.fr) and the French National Program
405 EC2CO-Biohefect "MACROFLUX". Finally, we thank the Karnataka Forest Department and
406 the staff of the Bandipur National Park for all the facilities and support they provided.
407
408 **Appendix A.** Supplementary data to this article can be found online at
409 Bardoni, D.; Meunier, J-D.; Jouquet, P., 2019, Phytoliths in termite mounds and in the soil
410 environment, India, 2017. https://doi.org/10.23708/G3HWON,
411 Jouquet, P.; Jamoteau, F.; Majumdar, S.; Nagabovanalli, P.; Caner, L.; Meunier, J-D., 2019,
412 Soil physical, chemical and mineralogical properties. Comparison between termite mounds
413 and the soil environment in Mule Hole, Karnataka, India, https://doi.org/10.23708/MHUF7F
414
415
416

417 **References**

418 Abe, S.S., Kotegawa, T., Onishi, T., Watanabe, Y., Wakatsuki, T., 2012. Soil particle
419 accumulation in termite (*Macrotermes bellicosus*) mounds and the implications for soil
420 particle dynamics. Ecol. Res. 27, 219-227.

421 Alexandre, A., Meunier, J.-D., Colin, F., Koud, J.-M., 1997. Plant impact on the
422 biogeochemical cycle of silicon and related weathering processes. Geochim. Cosmochim.
423 Ac. 61, 677–682.

424 Amadou Issoufou, A., Soumana, I., Maman, G., Konate, S., Mahamane, A., 2019. Effects of
425 termites growth on litter decomposition: a modeling approach. International Journal of
426 Recycling of Organic Waste in Agriculture, 1–7.

427 Andrade, F.A., Al-Qureshi, H.A., Hotza, D., 2011. Measuring the plasticity of clays: A review.
428 Appli. Clay Sci. 51, 1–7.

429 Barbiero, L., Parate, H. R., Descloitres, M., Bost, A., Furian, S., Kumar, M. S. M., Kumar, C.,
430 Braun, J.-J., 2007. Using a structural approach to identify relationships between soil and
431 erosion in a semi-humid forested area, South India. Catena 70, 313–329.

432 Baskaran, N., Balasubramanian, M., Swaminathan, S., Desai, A.A., 2010. Feeding ecology of
433 the Asian elephant Elephas maximus Linnaeus in the Nilgiri Biosphere Reserve, southern
434 India. Journal of the Bombay Natural History Society 107, 3.

435 Bottinelli, N., Jouquet, P., Capowiez, Y., Podwojewski, P., Grimaldi, M., Peng, X., 2015. Why
436 is the influence of soil macrofauna on soil structure only considered by soil ecologists?
437 Soil Till. Res. 146, 118–124.

438 Brady, N.C., Weil, R.R., 1999. The nature and properties of soils. Twelfth Edition. Upper
439 Saddle River, New Jersey, Practice Hall, 881p.

440 Braun, J.-J., Descloitres, M., Riotte, J., Deschamps, P., Violette, A., Marechal, J. C., Sekhar,
441 M., Kumar, M.S.M., Subramanian, S., 2009. Contemporary versus long-term weathering
442 rates in Tropics: Mule Hole, South India. Geochim. Cosmochim. Ac. 73, A157.

443 Bremond, L., Alexandre, A., Peyron, O., Guiot, J., 2008. Definition of grassland biomes from
444 phytoliths in West Africa. J. Biogeogr. 35, 2039–2048.
445 Caner, L., Radtke, L.M., Vignol-Lelarge, M.L., Inda, A.V., Bortoluzzi, E.C., Mexias, A.S.,
446 2014. Basalt and rhyo-dacite weathering and soil clay formation under subtropical climate
447 in southern Brazil. Geoderma 235, 100–112.
448 Carignan, J., Hild, P., Mevelle, G., Morel, J., Yeghicheyan, D., 2001. Routine analyses of trace
449 elements in geological samples using flow injection and low pressure on-line liquid
450 chromatography coupled to ICP-MS: a study of geochemical reference materials BR, DR-
451 N, UB-N, AN-G and GH. Geostandards Newsletter 25, 187–198.
452 Cheik, S., Bottinelli, N., Sukumar, R., Jouquet, P., 2018. Fungus-growing termite foraging
453 activity increases water infiltration but only slightly and temporally impacts soil physical
454 properties in southern Indian woodlands. Eur. J. Soil Biol. 89, 20–24.
455 Cheik, S., Shanbhag, R., Harit, A., Bottinelli, N., Sukumar, R., Jouquet, P., 2019. Linking
456 termite feeding preferences and soil physical functioning in Southern-Indian woodlands.
457 Insects 10, 4.
458 Chhotani, O.B., Bose, G., 1979. Nesting behaviour and nests of Indian termites. Zoologiana 2,
459 16–28.
460 Cornelis, J.-T., Titeux, H., Ranger, J., Delvaux, B., 2011. Identification and distribution of the
461 readily soluble silicon pool in a temperate forest soil below three distinct tree species.
462 Plant Soil 342, 369-378.
463 Cornelis, J.T., Delvaux, B., 2016. Soil processes drive the biological silicon feedback loop.
464 Funct. Ecol. 30, 1298–1310.
465 Datnoff, L.E., Seebold, K.W., Correa-V., F.J., 2001. The use of silicon for integrated disease
466 management: reducing fungicide applications and enhancing host plant resistance. In:
467 Studies in Plant Science, Elsevier. Vol. 8, pp: 171–184.

468 Erens, H., Mujinya, B.B., Mees, F., Baert, G., Boeckx, P., Malaisse, F., Van Ranst, E., 2015.
469 The origin and implications of variations in soil-related properties within Macrotermes
470 falciger mounds. Geoderma 249–250, 40-50.
471 Fraysse, F., Pokrovsky, O.S., Schott, J., Meunier, J-D., 2009. Surface chemistry and reactivity
472 of plant phytoliths in aqueous solutions. Chem. Geol. 258, 197–206.
473 Georgiadis, A., Marhan, S., Lattacher, A., Mäder, P., Rennert, T., 2019. Do earthworms affect
474 the fractionation of silicon in soil? Pedobiol. 75, 1–7.
475 Gilkes, R.J., McKenzie, R.M., 1988. Geochemistry and Mineralogy of Manganese in Soils. In:
476 Graham R.D., Hannam R.J., Uren N.C. (eds) Manganese in Soils and Plants.
477 Developments in Plant and Soil Sciences, Vol 33. Springer, Dordrecht.
478 Haysom, M.B.C., Chapman, L.S., 1975. Some aspects of the calcium silicate trials at Mackay.
479 Proceeding 42, 117–122
480 Holt, A.J., Lepage, M., 2000. Termites and soil properties. Termites: evolution, sociality,
481 symbioses, ecology. B. Abe T., D.E., Higashi, M.. Netherlands, Kluwer Academic
482 Publishers. 18, pp: 389–407.
483 International Committee for Phytolith Taxonomy (ICPT), 2019. International Code for
484 Phytolith Nomenclature (ICPN) 2.0, Ann. Bot-London, 124, 189–199.
485 IUSS-Working-Group-WRB, 2015. World reference base for soil resources 2014, update 2015:
486 International soil classification system for naming soils and creating legends for soil
487 maps. *World Soil Resources Reports No. 106*, 192.
488 Jouquet, P., Mamou, L., Lepage, M., Velde, B., 2002. Effect of termites on clay minerals in
489 tropical soils: fungus-growing termites as weathering agents. Eur. J. Soil Sci. 53, 521–
490 527.
491 Jouquet, P., Bottinelli, N., Lata, J-C., Mora, P., Caquineau, S., 2007. Role of the fungus-
492 growing termite *Pseudacanthotermes spiniger* (Isoptera, Macrotermitinae) in the

493 dynamic of clay and soil organic matter content. An experimental analysis. Geoderma
494 139, 127–133.
495 Jouquet, P., Traoré, S., Choosai, C., Hartmann, C., Bignell, D., 2011. Influence of termites on
496 ecosystem functioning. Ecosystem services provided by termites. Eur. J. Soil Biol. 47,
497 215–222.
498 Jouquet, P., Bottinelli, N., Shanbhag, R.R., Bourguignon, T., Traoré, S., Abbasi, S.A., 2016.
499 Termites: the neglected soil engineers of tropical soils. Soil Sci. 181, 157–165.
500 Jouquet, P., Guilleux, N., Caner, L., Chintakunta, S., Ameline, M., Shanbhag, R.R., 2016.
501 Influence of soil pedological properties on termite mound stability. Geoderma 262, 45–
502 51.
503 Jouquet, P., Airola, E., Guilleux, N., Harit, A., Chaudhary, E., Grellier, S., Riotte, J., 2017a.
504 Abundance and impact on soil properties of cathedral and lenticular termite mounds in
505 Southern Indian woodlands. Ecosystems 20, 769–780.
506 Jouquet, P., Caner, L., Bottinelli, N., Chaudhary, E., Cheik, S., Riotte, J., 2017. Where do
507 South-Indian termite mound soils come from? Appli. Soil Ecol. 117, 190–195.
508 Korndörfer, G.H., Lepsch, I., 2001. Effect of silicon on plant growth and crop yield. Studies in
509 plant science, Elsevier. 8, 133–147.
510 Lanson, B., 1997. Decomposition of experimental X-ray diffraction patterns (profile fitting): a
511 convenient way to study clay minerals. Clay Clay Miner. 45, 132–146.
512 Lavelle, P., Bignell, D., Lepage, M., 1997. Soil function in a changing world: the role of
513 invertebrate ecosystem engineers. Eur. J. Soil Biol. 33, 159–193.
514 Liang, Y., Nikolic, M., Bélanger, R., Gong, H., Song, A., 2015. Silicon in agriculture.
515 Dordrecht: Springer, 10: 978–994.

516 Loko, L.E.Y., Orobiyi, A., Agre, P., Dansi, A., Tamò, M., Roisin, Y., 2017. Farmers' perception
517 of termites in agriculture production and their indigenous utilization in Northwest Benin.
518 J. Ethnobiol. Ethnomed. 13, 64.
519 Lucas, Y., Luizao, F. J., Chauvel, A., Rouiller, J., Nahon, D., 1993. The relation between
520 biological activity of the rain forest and mineral composition of soils. Science 260, 521–
521 523.
522 Mehra, O.P., Jackson, M.L., 1960. Iron oxide removal from soils and clays by dithionite–citrate
523 systems buffered with sodium bicarbonate. Clays and Clay Minerals 7, 317–327.
524 Melzer, S.E., Knapp, A.K., Kirkman, K.P., Smith, M.D., Blair, J.M., Kelly, E.F., 2010. Fire
525 and grazing impacts on silica production and storage in grass dominated ecosystems.
526 Biogeochem. 97, 263–278.
527 Mujinya, B.B., Van Ranst, E., Verdoodt, A., Baert, G., Ngongo, L. M., 2010. Termite
528 bioturbation effects on electro-chemical properties of Ferralsols in the Upper Katanga
529 (DR Congo). Geoderma 158(3-4), 233-241.
530 Mujinya, B. B., Mees, F., Boeckx, P., Bodé, S., Baert, G., Erens, H., Delefortrie, S., Verdoodt,
531 A., Ngongo, M., Van Ranst, E., 2011. The origin of carbonates in termite mounds of the
532 Lubumbashi area, D.R. Congo. Geoderma 165(1), 95-105.
533 Mujinya, B.B., Mees, F., Erens, H., Dumon, M., Baert, G., Boeckx, P., Ngongo, M., Van Ranst,
534 E., 2013. Clay composition and properties in termite mounds of the Lubumbashi area,
535 D.R. Congo. Geoderma 192, 304-315.
536 Narayanaswamy, C., Prakash, N.B., 2009. Calibration and categorization of plant available
537 silicon in rice soils of South India. J. Plant Nut. 32, 1237–1254.
538 Narayanaswamy, C., Prakash, N.B., 2010. Evaluation of selected extractants for plant-available
539 silicon in rice soils of southern India. Commun. Soil Sci. Plan. 41, 977–989.

Oberst, S., Lai, J.C.S., Evans, T.A., 2016. Termites utilise clay to build structural supports and so increase foraging resources. Sci. Rep-UK 6, 20990.

Righi, D., Dinel, H., Schulten, H.R., Schnitzer, M., 1995. Characterization of clay-organic-matter complexes resistant to oxidation by peroxide. Eur. J. Soil Sci. 46, 423–429.

Riotte, J., Meunier, J-D., Zambardi, T., Audry, S., Barboni, D., Anupama, K., Prasad, S., Chmeleff, J., Poitrasson, F., Sekhar, M., 2018. Processes controlling silicon isotopic fractionation in a forested tropical watershed: Mule Hole Critical Zone Observatory (Southern India). Geochim. Cosmochim. Ac. 228, 301–319.

Sall, S., Brauman, A., Fall, S., Rouland, C., Miambi, E., Chotte, J.-L., 2002. Variation in the distribution of monosaccharides in soil fractions in the mounds of termites with different feeding habits (Senegal). Biol. Fertil. Soils 36, 232–239.

Sauer, D., Saccone, L., Conley, D.J., Herrmann, L., Sommer, M., 2006. Review of methodologies for extracting plant-available and amorphous Si from soils and aquatic sediments. Biogeochem. 80, 89–108.

Schaefer, C.E.R., 2001. Brazilian latosols and their B horizon microstructure as long-term biotic constructs. Austr. J Soil Res. 39, 909–926.

Schoelynck, J., Subalusky, A.L., Struyf, E., Dutton, C.L., Unzué-Belmonte, D., Van de Vijver, B., Post, D.M., Rosi, E.J., Meire, P., Frings, P., 2019. Hippos (*Hippopotamus amphibius*): The animal silicon pump. Science advances 5(5): eaav0395.

Schwertmann, U., 1964. Differenzierung der Eisenoxide des Bodens durch Ekstraktion mit saurer Ammoniumoxalat-Lösung. Zeitschrift für Pflanzenernährung und Bodenkdunde 105, 194–202.

Shanbhag, R.R., Sundararaj, R., 2013. Imported wood decomposition by termites in different agro-eco zones of India. Int. Biodeter. Biodegr. 85, 16–22.

565 Shanbhag, R.R., Kabbaj, M., Sundararaj, R., Jouquet, P., 2017. Rainfall and soil properties
566 influence termite mound abundance and height: A case study with *Odontotermes obesus*
567 (Macrotermitinae) mounds in the Indian Western Ghats forests. Appli. Soil Ecol. 111,
568 33–38.
569 Shanbhag, R.R., Harit, A., Cheik, S., Chaudhary, E., Bottinelli, N., Sundararaj, R., Jouquet, P.,
570 2019. Litter Quality Affects Termite Sheeting Production and Water Infiltration in the
571 Soil. Sociobiol. 66, 491–499.
572 Singer, M.J., Munns, D.N., 1999. Acidity and salinity. Soils: An Introduction. Upper Saddle
573 River, NJ, Prentice-Hall, pp. 285–296.
574 Soil Survey Staff, 2014. Keys to Soil Taxonomy - Soil Survey Staff, Twelfth Edition. US
575 Department of Agriculture, Washington D.C.
576 Sommer, M., Kaczorek, D., Kuzyakov, Y., Breuer, J., 2006. Silicon pools and fluxes in soils
577 and landscapes—a review. J. Plant Nutr. Soil Sci. 169, 310–329.
578 Spagnoli, G., Sridharan, A., Oreste, P., Bellato, D., Di Matteo, L., 2018. Statistical variability
579 of the correlation plasticity index versus liquid limit for smectite and kaolinite. Appl. Clay
580 Sci. 156, 152–159.
581 Suchéras-Marx, B., Escarguel, G., Ferreira, J., Hammer, Ø., 2019. Statistical confidence
582 intervals for relative abundances and abundance-based ratios: Simple practical solutions
583 for an old overlooked question. Mar. Micropaleontol. 151, 101751
584 Traore, S., Tigabu, M., Jouquet, P., Ouedraogo, S. J., Guinko, S., Lepage, M., 2015. Long-term
585 effects of *Macrotermes* termites, herbivores and annual early fire on woody undergrowth
586 community in Sudanian woodland, Burkina Faso. Flora 211: 40–50.
587 Traoré, S., Bottinelli, N., Aroui, H., Harit, A., Jouquet, P., 2019. Termite mounds impact soil
588 hydrostructural properties in southern Indian tropical forests. Pedobiol. 74, 1–6.

589 Vandevenne, F.I., Barão, L., Ronchi, B., Govers, G., Meire, P., Kelly, E. F., Struyf, E., 2015.
590 Silicon pools in human impacted soils of temperate zones. Global Biogeochem. Cy. 29,
591 1439–1450.
592 Velde, B., 2001. Clay minerals in the agricultural surface soils in the Central United States.
593 Clay Miner. 36, 277–294.
594 Violette, A., Goddéris, Y., Maréchal, J.-C., Riotte, J., Oliva, P., Kumar, M.S.M., Sekhar, M.,
595 Braun, J.-J., 2010. Modelling the chemical weathering fluxes at the watershed scale in the
596 Tropics (Mule Hole, South India): Relative contribution of the smectite/kaolinite
597 assemblage versus primary minerals. Chem. Geol. 277, 42-60.
598 Wielemaker, W.G., 1984. Soil formation by termites: a study in the Kisii area, Kenya (Doctoral
599 dissertation, Wielemaker).

600 **Figures and table captions**

601

602 Figure 1. Biplot showing the principal components analysis (PCA) from variables describing
603 soil physical and chemical properties showed in Table 1 and significantly influenced
604 by the different treatments: control soil sampled at 0-5 and 70-120 cm depth in blue
605 and yellow, respectively, and the termite mound soil (TM, in red) or the soil eroded
606 from the mound (EROD, in grey).

607

608 Figure 2. Clay content along the soil profile, in the outer part of termite mound (TM, arbitrary
609 displayed at + 50cm depth) and in the soil eroded from TM (EROD, arbitrary
610 displayed at + 5 cm depth). The three different soil profiles are given in three different
611 soil colors.

612

613 Figure 3. Histograms showing the percentages in SiO_2 and phytoliths (%), and the amounts in
614 Si_{CC} and Si_{AA} (ppm) in the outer part of termite mound (TM), in the soil eroded from
615 TM (EROD) and in the control soils at 0-5 and 70-120 cm depths ($Ctrl_{0-5}$ and $Ctrl_{70-120}$, respectively). Bars represent standard errors and histograms with the same letters
616
617 are not significantly different.

618

619 Figure 4. Abundance and diversity of phytoliths.
620 (a) Histograms showing the relative abundances of phytoliths in termite mound (TM)
621 and control samples at 0-5 ($Ctrl_{0-5}$) and 70-120 ($Crtl_{70-120}$) cm depths. The
622 differentiation was made into forest indicators, grasses, ND-elongate and ND-blocky
623 phytoliths.
624 (b) Ratio of spheroid decorated versus the sum of grass silica short cells (or D/P°
625 index).

626

627 Figure 5. Proportion of corroded, non-corroded and undetermined phytoliths for termite
628 mound (TM) and in the soil sampled at 0-5, 20-40 and 70-120 cm depths ($Ctrl_{0-5}$ and
629 $Ctrl_{70-120}$).

630

631 Figure 6. Examples of blocky and elongated non-corroded (a, b) and corroded phytoliths (c, d)
632 obtained in the microscope. The scale is given with the horizontal bar which
633 represents 40 mm.

634

635 Figure 7. Biplot showing the principal components analysis (PCA) from variables describing
636 clay mineralogy of the different soil materials. Treatments are the soil at 0-5 and 70-
637 120 cm depth (in blue and yellow, respectively), the soil from termite mound (TM,
638 in red) and the soil eroded from TM (EROD, in grey). Clays are kaolinite (K), well
639 crystallized illite (WCI), poorly crystallised illite (PCI), inters-stratified (IS) and
640 smectite (S).

641

642 Supplementary file 1. Percentage in Fe_2O_3 and Al_2O_3 along the soil profile, in the outer part of
643 termite mound (TM, arbitrary displayed at + 50 cm depth) and in the soil eroded from
644 TM (EROD, arbitrary displayed at + 5 cm depth).

645

646 Supplementary file 2. Percentage of well crystallized oxides in soil ($Fe_{DCB} - Fe_O$ and $Al_{DCB} -$
647 Al_O) extracted by the DCB (Fe_{DCB} and Al_{DCB}) and oxalate methods (Fe_O and Al_O)
648 (Mehra and Jackson, 1960; Schwertmann, 1964) along the soil profile, in the outer
649 part of termite mound (TM, arbitrary displayed at + 50 cm depth) and in the soil
650 eroded from TM (EROD, arbitrary displayed at + 5 cm depth).

Figure 1

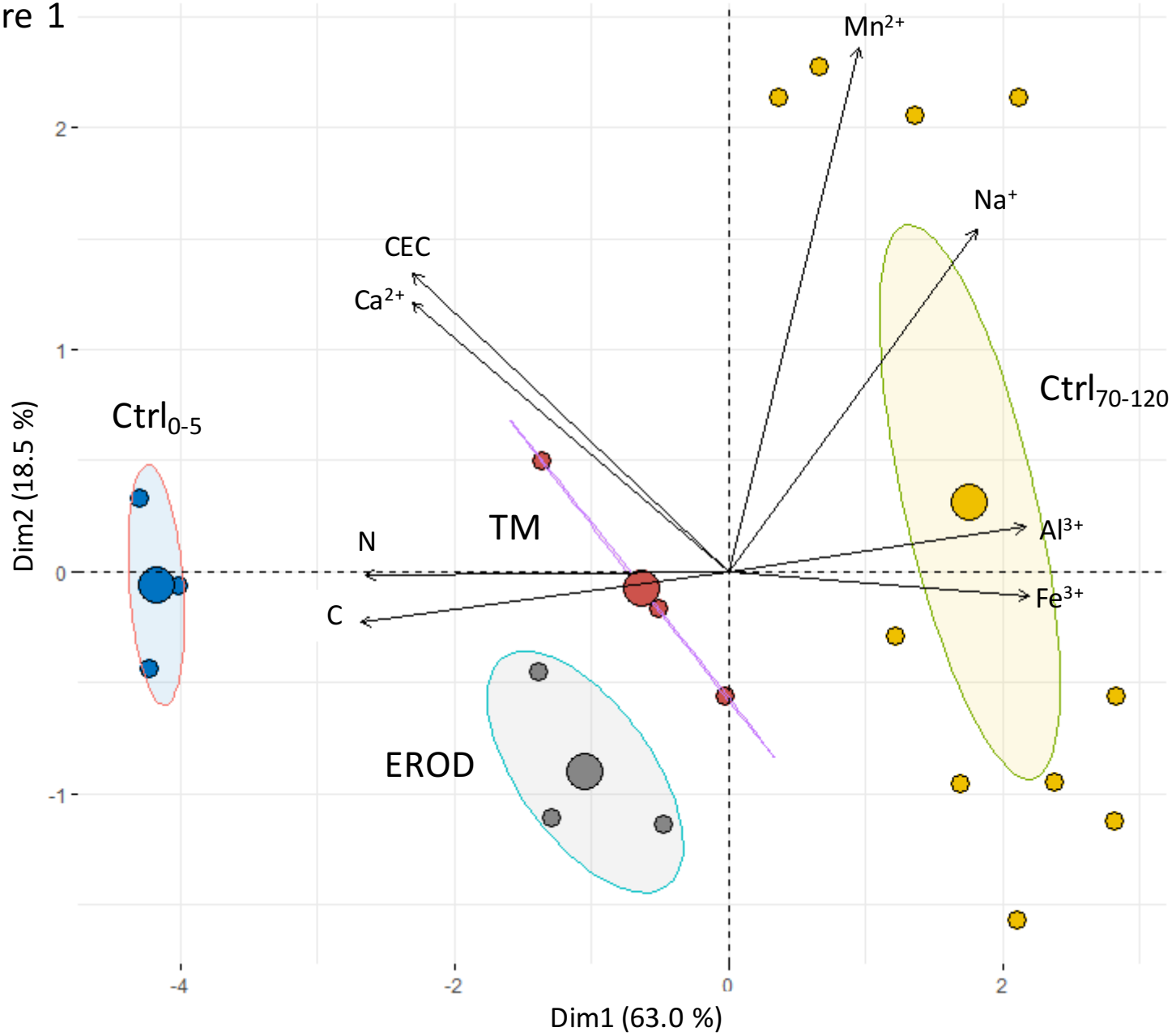
Mn2+
Na+
CEC
Ca2+
Ctrl70-120
Ctrl0-5
TM
N
Al3+
Fe3+
C
EROD
Dim2 (18.5 %)
Dim1 (63.0 %)
2
1
0
-1
-4
-2
0
2

Figure 2

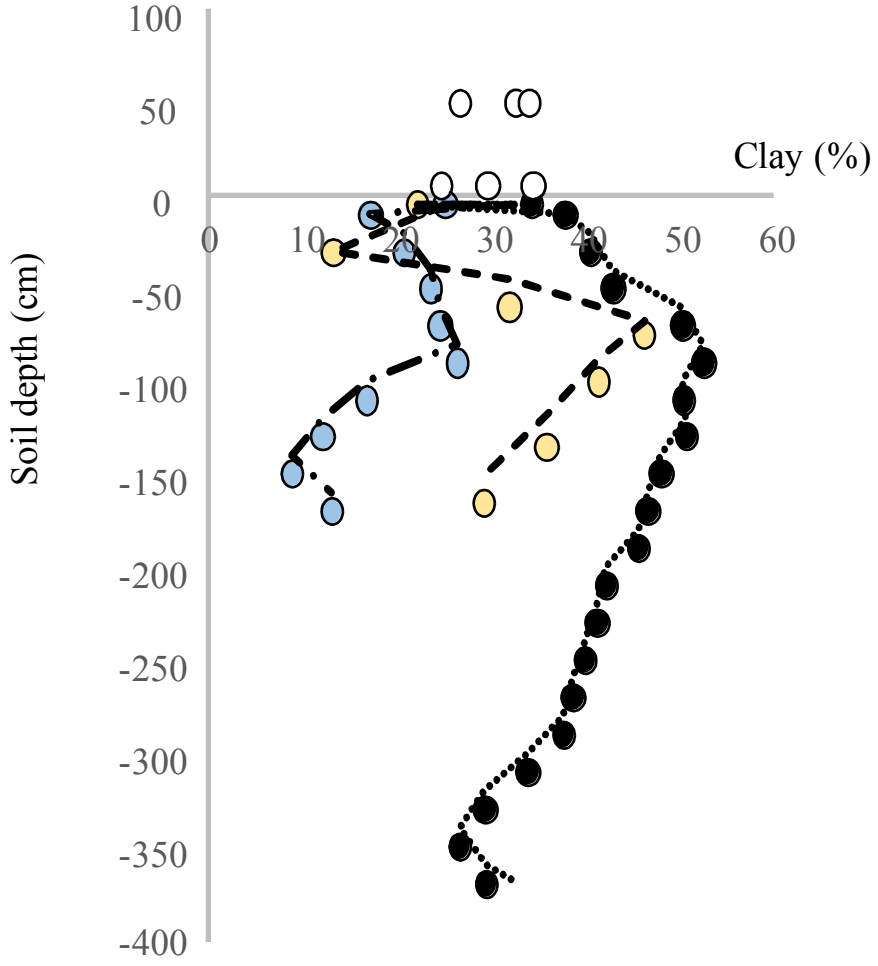
100
50
0
-50
-100
-150
-200
-250
-300
-350
-400
0
10
20
30
40
50
60
Clay (%)
Soil depth (cm)

Figure 3

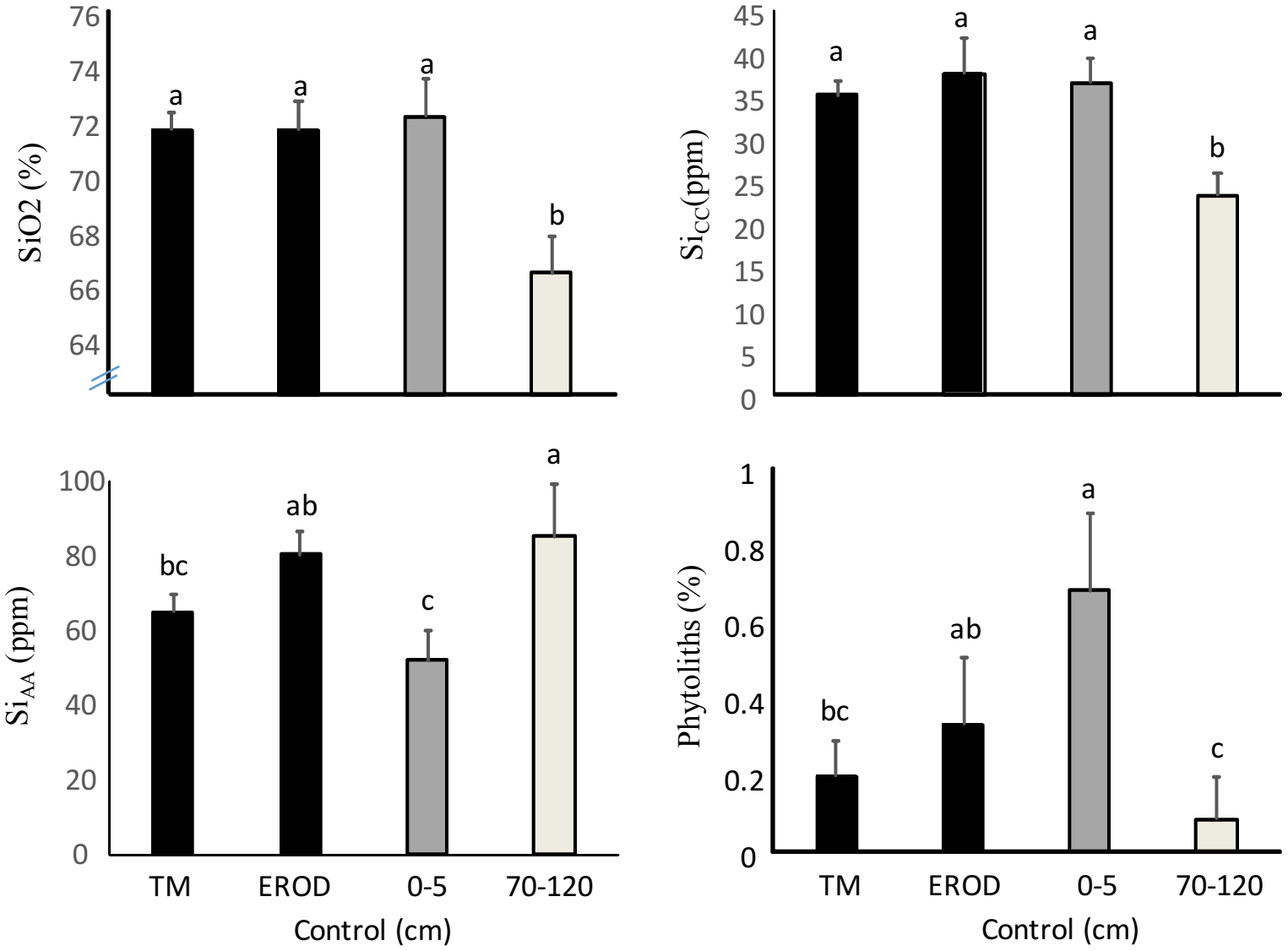
SiO2 (%)
76
74
72
70
68
66
64
a
a
a
b
Si_{CC}(ppm)
45
40
35
30
25
20
15
10
5
0
a
a
a
b
Si_{AA} (ppm)
100
80
60
40
20
0
bc
ab
c
a
Phytoliths (%)
1
0.8
0.6
0.4
0.2
0
bc
ab
a
c
TM
EROD
0-5
70-120
Control (cm)

Figure 4

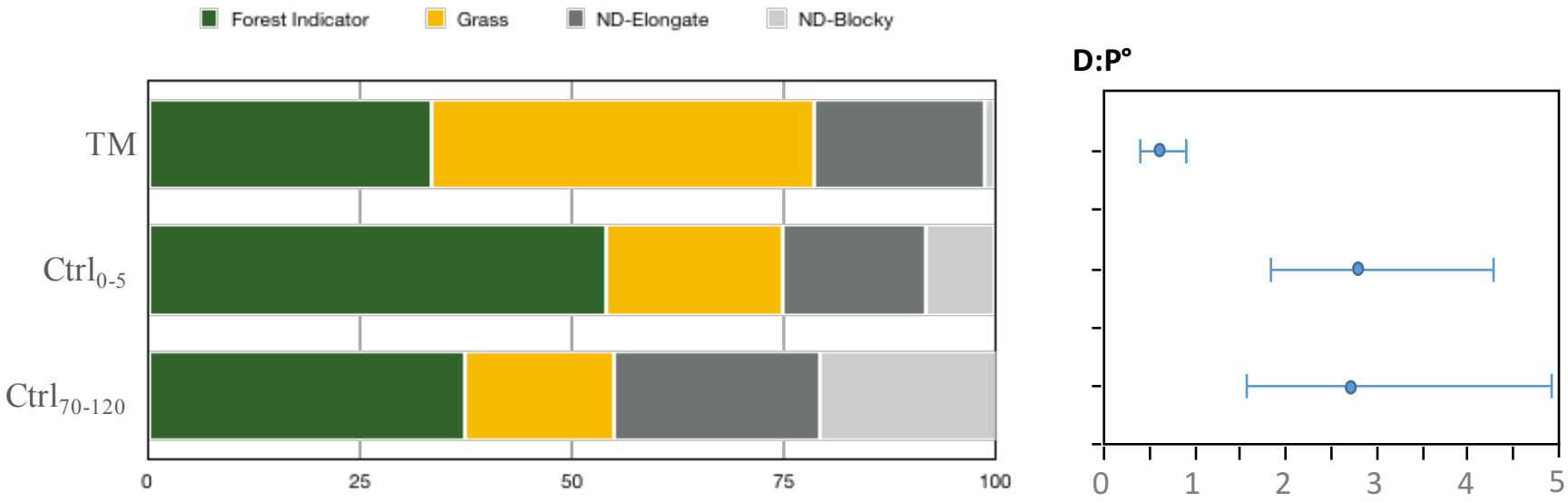
Forest Indicator
Grass
ND-Elongate
ND-Blocky
TM
Ctrl0-5
Ctrl70-120
0
25
50
75
100
D:P°
0
1
2
3
4
5

Figure 5

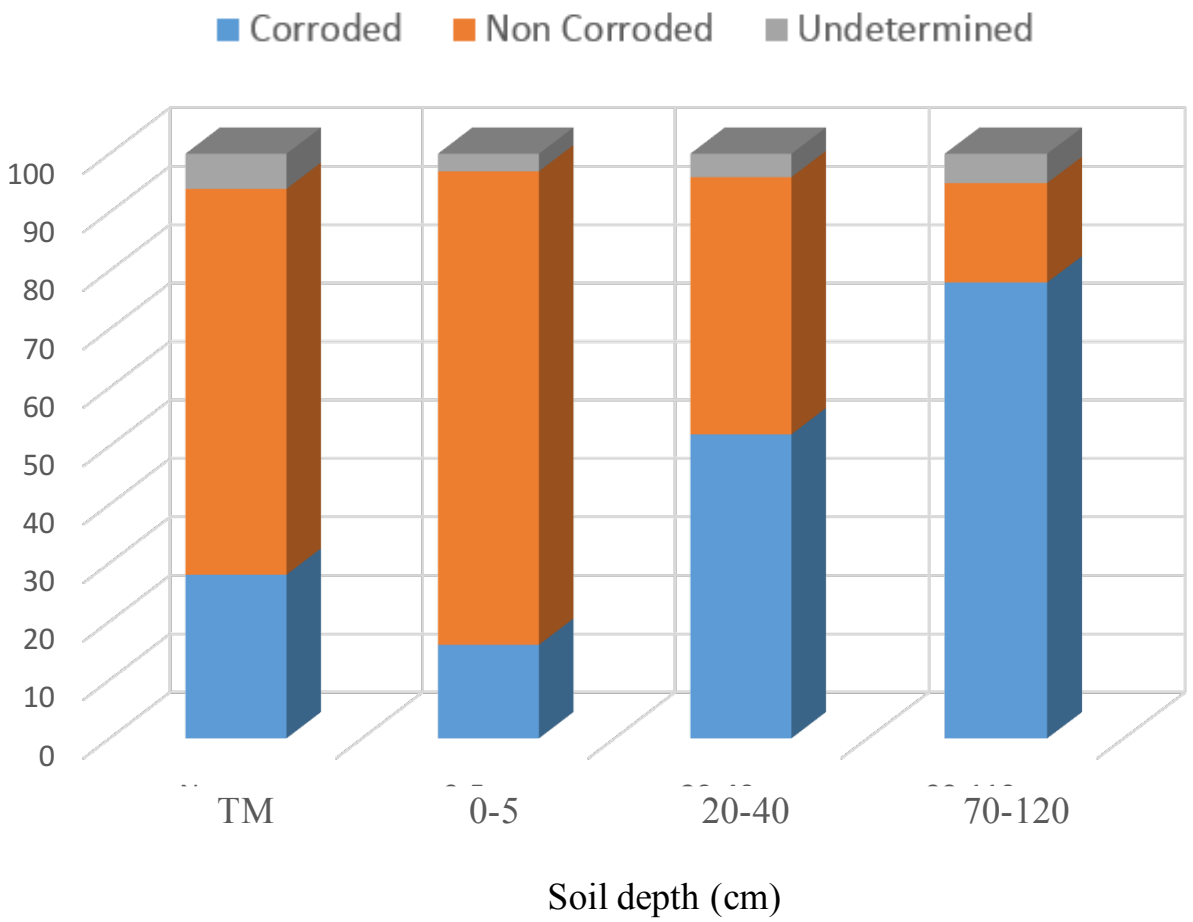
Corroded
Non Corroded
Undetermined
100
90
80
70
60
50
40
30
20
10
0
TM
0-5
20-40
70-120
Soil depth (cm)

Figure 6

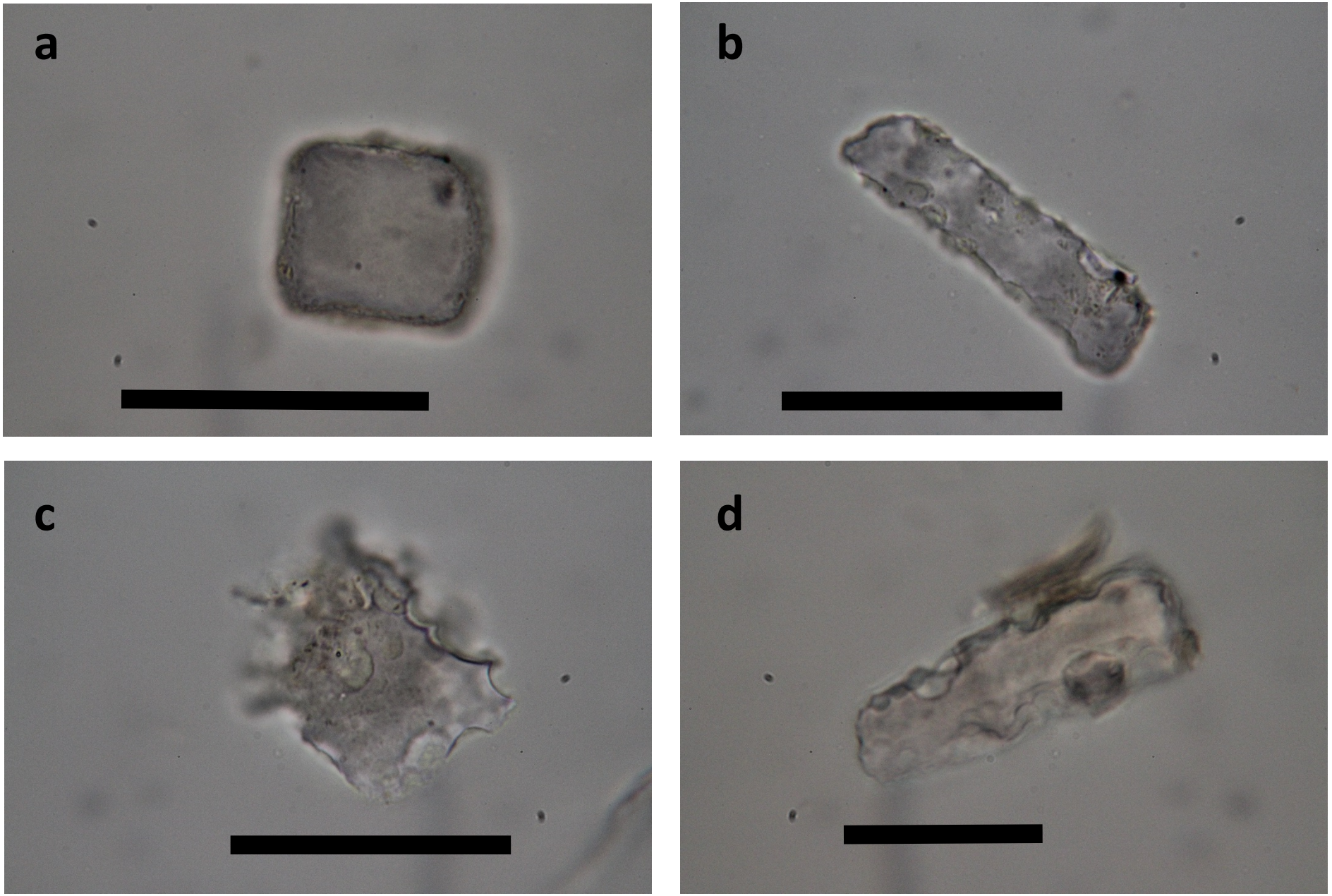

Figure 7

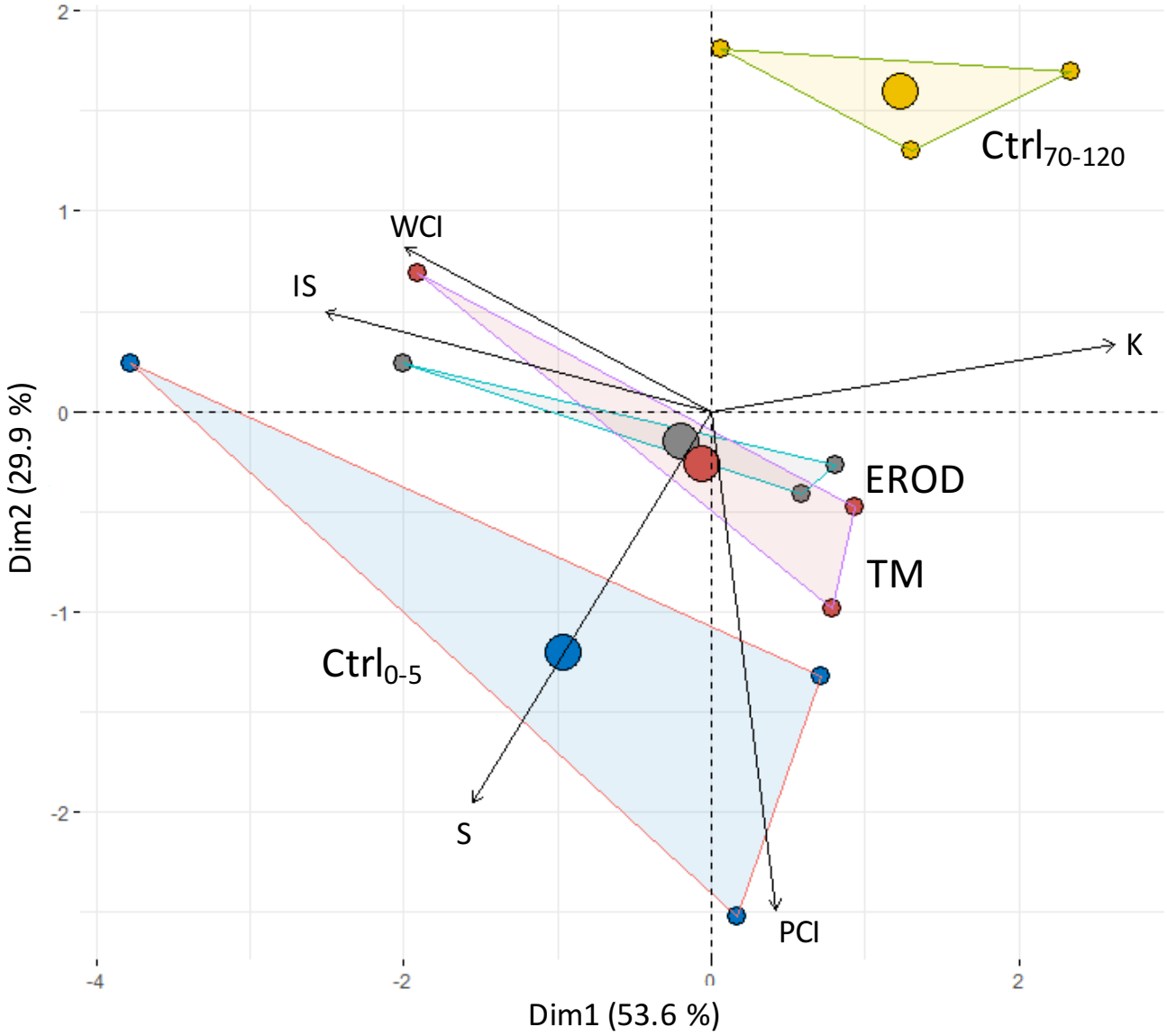
Ctrl70-120
WCI
IS
K
EROD
TM
Ctrl0-5
S
PCI
Dim2 (29.9 %)
Dim1 (53.6 %)
2
1
0
-1
-2
-4
-2
0
2

Supplementary file 1

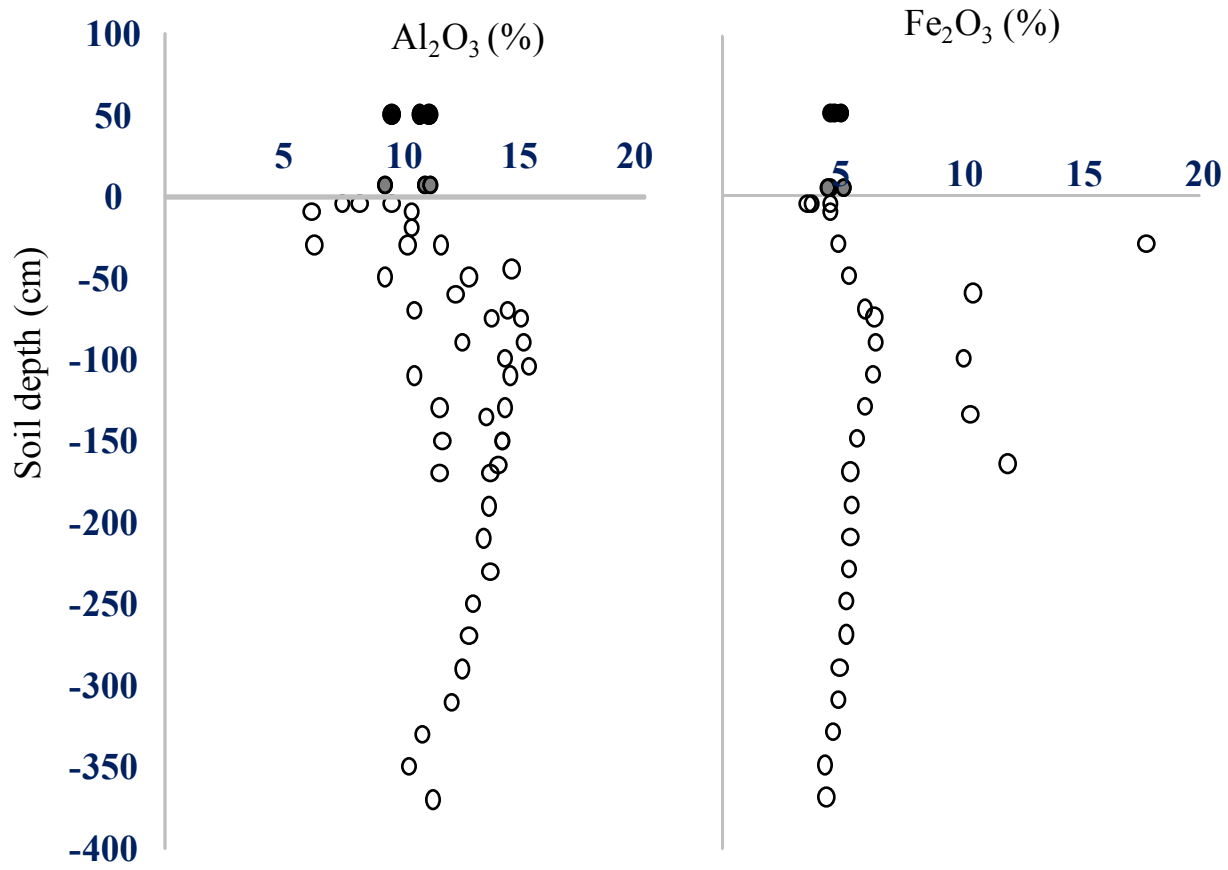

Supplementary file 2

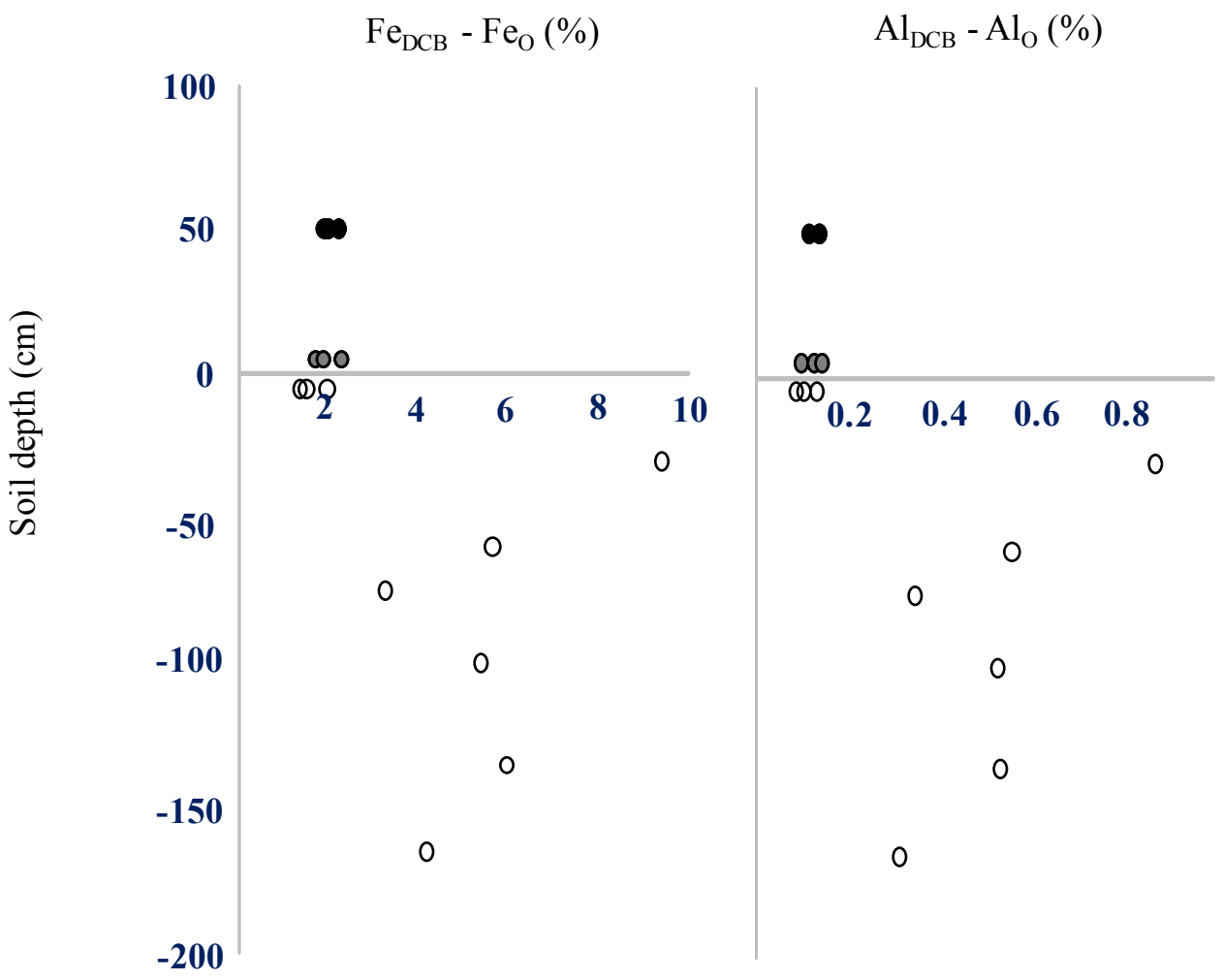

Table 1 Major physical (contents in clay, silt and sand, in %) and chemical properties (contents in C and N in %, CEC, Ca^{2+}, Mg^{2+}, Na^{+}, K^{+}, Fe^{3+}, Mn^{2+} and Al^{3+} in $cmol^{(+)}\,kg^{-1}$) in the control soils at 0-5 and 70-120 cm depth ($Ctrl_{0-5}$ and $Ctrl_{70-120}$, respectively) and in termite mound (TM) or the soil eroded from TM (EROD). Values in parentheses are standard errors, values with the same letter are similar at $P = 0.05$. Results from the ANOVA (F and P-values) and Wilcoxon–Mann–Whitney U (Chi^2 and P-values) tests are also given.

	C	N	Clay	Silt	Sand	CEC	Ca^{2+}	Mg^{2+}	Na^{+}	K^{+}	Fe^{3+}	Mn^{2+}	Al^{3+}	pH
			(%)						($cmol^{(+)}\,kg^{-1}$)					
TM	1.75^{b}	0.13^{b}	31.2	18.1	50.7	13.30^{b}	9.25^{b}	2.96	0.043^{b}	0.27	0.016^{ab}	0.18^{a}	0.09^{a}	6.03
(n = 3)	(0.38)	(0.03)	(3.87)	(0.6)	(1.8)	(0.61)	(0.60)	(0.05)	(0.002)	(0.04)	(0.001)	(0.03)	(0.01)	(0.07)
EROD	1.95^{b}	0.14^{b}	29.7	18.9	51.4	13.80^{b}	9.68^{b}	3.22	0.039^{b}	0.40	0.016^{ab}	0.04^{b}	0.09^{a}	6.45
(n = 3)	(0.30)	(0.02)	(4.85)	(0.2)	(2.6)	(0.25)	(0.21)	(0.12)	(0.009)	(0.06)	(0.002)	(0.01)	(0.01)	(0.22)
$Ctrl_{0-5}$	3.43^{a}	0.25^{a}	26.6	17.4	56.0	19.50^{a}	14.83^{a}	3.40	0.025^{b}	0.47	0.010^{b}	0.02^{b}	0.05^{b}	6.23
(n = 3)	(0.29)	(0.03)	(5.14)	(0.3)	(2.9)	(0.78)	(0.92)	(0.21)	(0.003)	(0.11)	(0.003)	(0.03)	(0.01)	(0.13)
$Ctrl_{70-120}$	0.49^{c}	0.05^{c}	37.23	18.06	44.72	11.78^{b}	8.00^{b}	3.36	0.111^{a}	0.49	0.022^{a}	0.16^{a}	0.13^{a}	6.75
(n = 10)	(0.27)	(0.03)	(14.87)	(2.02)	(3.17)	(1.11)	(0.89)	(0.34)	(0.01)	(0.09)	(0.002)	(0.04)	(0.01)	(0.90)
$F_{3,15}$	15.75	52.27	0.80	0.05	1.74	5.84	6.9		11.36	1.85	5.34	5.62	5.94	1.88
P	<0.001	<0.001	0.511	0.986	0.202	0.007	0.004		<0.001	0.182	0.010	0.008	0.007	0.222
	***	***				**	**		***		*	**	**	
Chi^2								1.08						
P								0.781						